Highly spin-polarized Dirac fermions at the graphene/Co interface

D. Marchenko,* A. Varykhalov, J. Sánchez-Barriga, and O. Rader
Helmholtz-Zentrum Berlin für Materialien und Energie, Elektronenspeicherring BESSY II, Albert-Einstein-Straße 15, 12489 Berlin, Germany

C. Carbone
Istituto di Struttura della Materia, Consiglio Nazionale delle Ricerche, Basovizza, 34149 Trieste, Italy

G. Bihlmayer
Peter Grünberg Institut and Institute for Advanced Simulation, Forschungszentrum Jülich and JARA, 52425 Jülich, Germany
(Received 18 February 2015; revised manuscript received 13 May 2015; published 18 June 2015)

The interface of graphene with ferromagnets is highly relevant for spintronics, because graphene on Co(0001) shows a largely intact Dirac cone and strong hybridization with Co 3*d* states breaking the sublattice symmetry that had been considered mutually exclusive. Here we show by spin- and angle-resolved photoemission that the Dirac cone and Dirac point are also highly spin polarized ($\sim -25\%$), which reinforces the puzzling issue of a strong graphene-substrate interaction. The problem is solved by our *ab initio* calculations which show that (i) the upper and lower halves of the Dirac cone belong to different sublattices and (ii) one half is spin polarized by spin-dependent hybridization because it is situated at the edge of a minority-spin band gap of the Co substrate.

DOI: 10.1103/PhysRevB.91.235431 PACS number(s): 73.22.Pr, 75.70.−i, 81.05.ue, 85.75.−d

Owing to its low spin-orbit interaction and resulting micrometer-range spin-relaxation length [1–4], graphene is considered a prime material for spin transport. Spin is typically injected from ferromagnetic contacts which make the graphene-ferromagnet interface and ferromagnetic graphene important subjects of investigation. Proximity magnetization of the graphene occurs by impurities [5] and at the interfaces [6]. The spin-filter properties of graphene interfaces with Ni and Co have been investigated by density functional theory, and 100% magnetoresistance was found [6]. Spin currents are reversible by electric gating [7]. For ferromagnetic graphene induced by a proximity magnetization, a spin superconductor state has been investigated theoretically [8]. In that case, intact spin-split Dirac cones of the ferromagnetic graphene enable the formation of electron-hole pairs which are spin polarized and may form an exciton condensate that can be charge insulating [9]. Calculations predict that graphene would acquire a ferromagnetic spin polarization of the Dirac cone of ∼24% when grown on the low-temperature ferromagnetic insulator EuO [10].

It has been difficult to detect ferromagnetic order in graphene. Primarily, it has been reported based on x-ray magnetic circular dichroism (XMCD) measurements at the carbon *K* edge, for example, for graphite-Fe multilayers [11], chemically functionalized graphene [12], and graphene on Ni [13]. In addition, the fate of the graphene Dirac cone and the associated transport properties in proximity magnetized graphene remains unclear because strong proximity magnetization principally also means strong electronic hybridization. The Dirac cone was found to be destroyed by a graphene-Ni interaction, and it was suggested that a monatomic layer of Cu in between graphene and Ni is required to restore the Dirac cone in graphene [6]. This Cu layer only slightly affects the magnetoresistance, but it strongly reduces the induced ferromagnetism in the graphene.

A strong ferromagnetic exchange interaction induced in graphene is also crucial for realizing the quantum anomalous Hall effect in graphene [14–18]. This topological quantum phase leads to edge states with a robust quantized Hall conductance $\sigma_{xy} = Ce^2/h$ (Chern number C). Both the spin-orbit interaction and the exchange interaction have to be provided by proximity effects.

Interfacing graphene with the heavy metals Au [19] and Ir [20] under preservation of the Dirac cone has been achieved, probably because breaking of the graphene sublattice symmetry is avoided by a large-scale moiré superstructure and a large graphene-substrate distance in both cases [21]. The resulting proximity spin-orbit interaction is giant sized on Au (∼100 meV [22]) and Ir (∼50 meV [23]). Because the inversion symmetry perpendicular to the graphene plane is broken by the proximity effect, the spin-orbit effect is of Rashba type, which leads graphene to the peculiar spin texture sketched in Fig. 1(a) [24,25].

Figure 1(b) shows, for comparison, the spin texture of a ferromagnetic Dirac cone. It has been widely believed that on ferromagnets Ni and Co—which present a much higher electronic density of states at the Fermi level and on which the graphene layer is closer by 1 Å than on Au and Ir—preserving the Dirac cone is hopeless. Moreover the graphene adsorption site is "on top" and breaks the graphene sublattice symmetry maximally.

In this situation, it came as a surprise that strong hybridization and an intact Dirac cone are instead compatible [26]. This was demonstrated by angle-resolved photoemission (ARPES) for graphene on Ni(111) and Co(0001). In the measured band structure, the strong interaction between the graphene and its substrate does not lead to a gapped Dirac point as expected for a $p(1 \times 1)$ "on-top" adsorbed graphene ($\mathcal{AC}$ stacking). Instead, the gap occurs away from the Dirac point where the π and 3*d* bands have an anticrossing. The Dirac point itself becomes shifted to a higher binding energy and remains intact

*Present address: Physikalische und Theoretische Chemie, Freie Universität Berlin, Takustraße 3, 14195 Berlin, Germany.

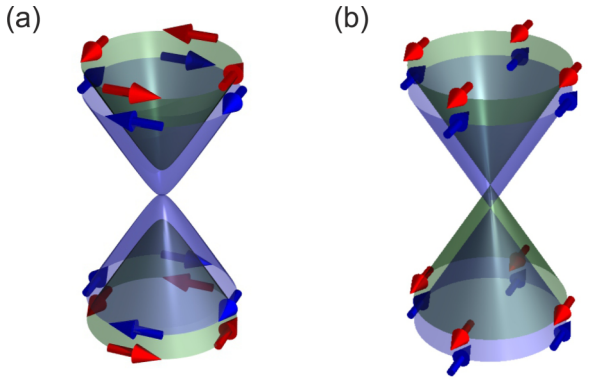

FIG. 1. (Color online) Comparison of (a) spin-orbit and (b) exchange-type spin splittings applied to the graphene Dirac cone dispersion.

in the ARPES experiment. Density functional theory (DFT) calculations of graphene on Ni identify that it has a counterpart in the unoccupied states [26].

The question arises now whether the induced spin polarization indicated by XMCD for graphene/Ni is only limited to the immediate hybridization region, or are the Dirac point and the linear portion of the π band also spin polarized. Before the discovery of the intact Dirac point, spin-resolved photoemission of the π band had already been performed away from the Dirac point: For graphene/Co(0001) it gave hardly any spin polarization P [27] and for graphene/Ni(111) it gave values of $P = (0 \pm 2)\%$ [27] and $P = -12\%$ [28] at different points in the Brillouin zone.

In the present work we have chosen Co(0001) for graphene growth. Using spin- and angle-resolved photoemission measurements, we demonstrate strong spin polarization and spin splitting of the graphene Dirac cone. We explicitly distinguish the exchange from spin-orbit effects in the experiment. We distinguish graphene from Co states by their symmetry and show that the Dirac point and its spin polarization are not simply due to states of the Co substrate. The calculation confirms this assignment and shows that the Dirac cone and Dirac point are situated in a minority-spin bulk band gap of the Co.

Graphene has been grown on 20 atomic layers of Co on W(110), as described before [26]. Spin- and angle-resolved photoemission measurements have been performed with a hemispherical energy analyzer equipped with a Rice University Mott-type spin detector [29]. Experiments have been conducted using linearly polarized synchrotron radiation of 62 eV photon energy. Before each set of measurements the sample has been magnetized in the in-plane $\overline{\Gamma M}$ direction using a Helmholtz coil. The spin detector zero asymmetry has been calibrated by selecting the level where spin asymmetries for two opposite magnetizations coincide. More information is given elsewhere [30,31].

Our theoretical results were obtained by the full-potential linearized augmented plane wave method in the generalized gradient approximation to DFT using the FLEUR code [32]. Structural optimization of graphene on a 14-layer Co film has been applied to the topmost three layers, allowing also for a buckling due to the two inequivalent sublattice sites of the graphene in the $p(1 \times 1)$ "on-top" geometry. The results

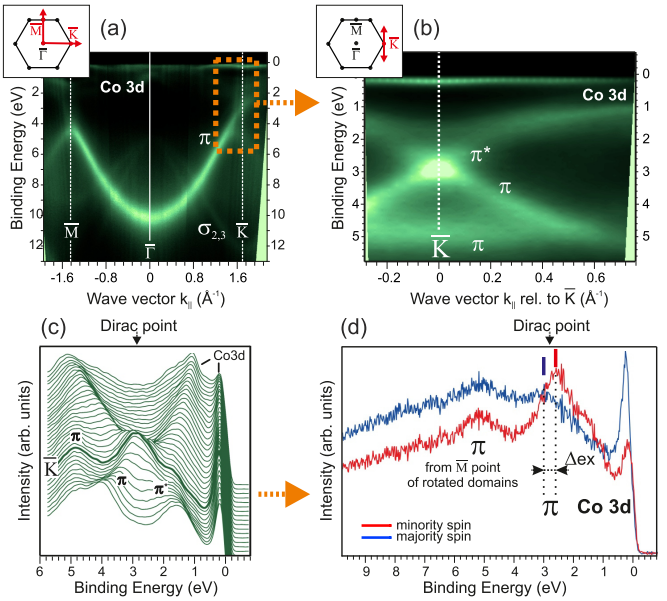

FIG. 2. (Color online) Spin- and angle-resolved photoemission from epitaxial graphene/Co(0001). (a) Valence band overview in the $\overline{\Gamma K}$ and $\overline{\Gamma M}$ directions. (b) The graphene Dirac cone region measured perpendicular to $\overline{\Gamma K}$ through the $\overline{K}$ point of the graphene Brillouin zone. (c) shows data from (b) as a stack of spectra. (d) Spin-resolved measurement conducted exactly at the $\overline{K}$ point. Red and blue spectra correspond to the minority and majority spin, respectively.

shown are for a structure with the average distance reduced to 2.05 Å due to van der Waals interactions [33] and retaining a buckling of 0.01 Å with the spin-orbit coupling effects included.

Figure 2(a) shows an ARPES overview along the $\overline{\Gamma M}$ and $\overline{\Gamma K}$ directions of the graphene Brillouin zone. Due to the strong graphene-Co interaction, the characteristic graphene π-band dispersion is shifted to higher binding energies compared to freestanding graphene [19]. The photoemission intensity of the π band is strongly modulated, so that after crossing the $\overline{K}$ point, the π band is no longer visible when measured along $\overline{\Gamma K}$ [34,35]. When measured in the direction perpendicular to $\overline{\Gamma K}$ through the $\overline{K}$ point, both sides of the Dirac cone are clearly visible [see Figs. 2(b) and 2(c)]. This is the experimental geometry used in all subsequent figures. The Dirac point in spin-integrated photoemission is seen at 2.8 eV binding energy. Near the Fermi level there are slightly dispersing Co states; the upper part of the graphene Dirac cone hybridizes with the Co states in that region. Besides the graphene Dirac cone dispersion, in addition, there is a faint band around 5.2 eV binding energy. It originates from the same π band but the $\overline{M}$ point of the rotated graphene domains [26]. Growth has recently been improved so that contributions from rotated domains disappear from the spectra [36].

Figure 2(d) shows spin-resolved measurement exactly at the $\overline{K}$ point of the graphene Brillouin zone. Majority- ($I^{\uparrow}$) and minority-spin photoemission intensities ($I^{\downarrow}$) are clearly identified by the background spin polarization at higher binding energy. A strong difference between intensities, meaning a strong spin polarization $P = (I^{\uparrow} - I^{\downarrow})/(I^{\uparrow} + I^{\downarrow})$, occurs everywhere in the spectrum in Fig. 2(d): the

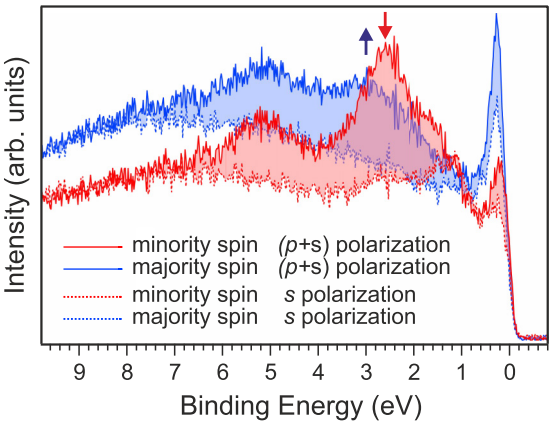

FIG. 3. (Color online) Effect of incident light polarization. The red shaded area shows the difference in the minority-spin spectra for $(p+s)$ and pure s polarization of the incident light. The blue shaded area is for the difference in majority-spin spectra.

background (featureless at 6 eV and higher binding energies), Co-derived states, and the graphene Dirac point which appears as a minority-spin peak at 2.6 eV. The spin polarization as measured at the Dirac point is about -10% and has a minority-spin character, and the background spin polarization is about $+15\%$ so that the Dirac point spin polarization relative to the background polarization is about -25%. In the majority-spin spectrum there is also a broad peak around 3 eV binding energy, which can be assigned as the majority-spin counterpart of the Dirac point.

We want to verify that the minority-spin peak at 2.6 eV originates from the graphene. The orbital responsible for the graphene π band and the Dirac cone is a p_z orbital pointing perpendicularly to the graphene plane. Figure 3 shows the influence of the incident-light polarization on the spin-resolved spectra at $\overline{K}$. Here $(p+s)$ polarization excites both σ and p_z graphene orbitals. The π-band intensity dominates the valence band in this case. s-polarized incident photons suppress photoemission from the p_z orbitals and thus from the Dirac cone. The difference is presented in Fig. 3 as shaded areas. Note that the Co intensities also depend on the light polarization, but they are large only in the energy region about 2 eV from the Fermi level with a small minority-spin feature at 2.3 eV. (See the measurement of pure Co(0001) [30,31].) This means that the shaded areas correspond predominantly to the graphene π-band intensity, and that the minority-spin polarization at 2.6 eV and the majority-spin polarization at $\sim$3 eV and the splitting between them in fact belong to the graphene Dirac cone.

Figures 4(a), 4(c), 4(e), and 4(g) (left panels) show the graphene Dirac cone dispersion measured with spin resolution. Going away from the $\overline{K}$ point, the minority-spin π band splits into two bands, i.e., upper π^* and lower π branches of the Dirac cone. The lower branch can be followed in the minority-spin spectra, although the feature progressively broadens and loses intensity. Already at about 0.3 Å^{-1} the upper branch mixes and hybridizes with Co $3d$ states, so that at 0.7 Å^{-1} the peak around 1.2 eV binding energy can be solely attributed to a minority-spin Co $3d$ state. Dispersion of the majority-spin part of the Dirac cone is not distinguishable from the background due to its large broadening and low intensity. Figure 4(d) shows

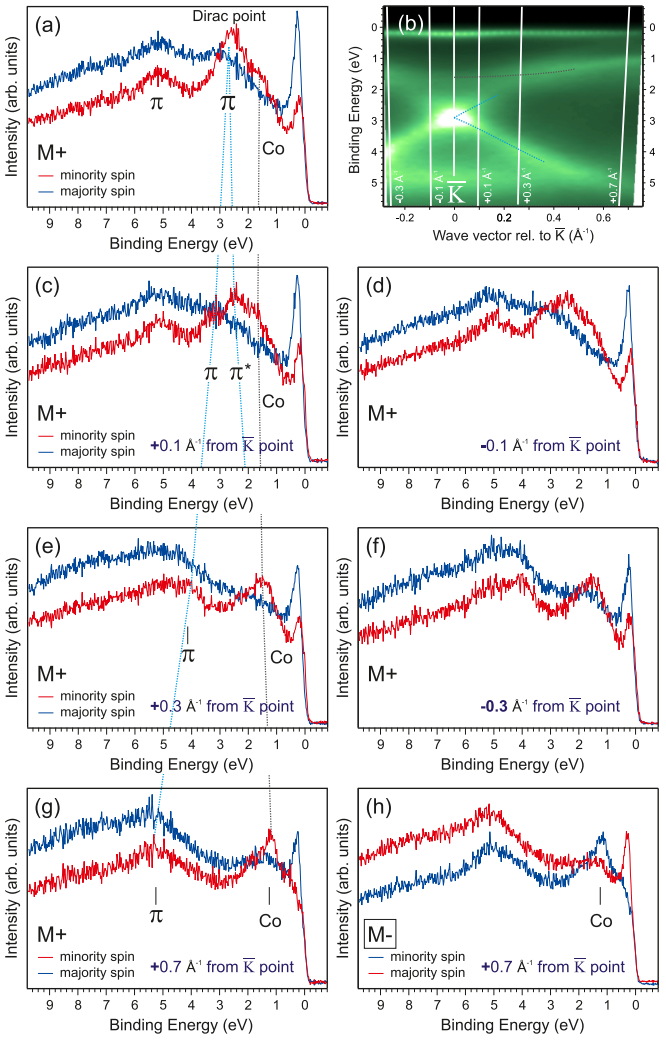

FIG. 4. (Color online) (b) shows the Dirac cone dispersion and positions of spin-resolved measurements. Left column panels [(a), (c), (e), (g)] show the Dirac cone dispersion obtained with spin resolution, going from 0 to +0.7 Å^{-1} relative to the $\overline{K}$ point. (d) and (f) are measurements for opposite wave vectors to those shown in (c) and (e). They show that there is no spin-orbit contribution to the observed Dirac cone spin polarization. (h) Reversal of the spin-resolved spectrum (g) when the sample magnetization direction is reversed.

a spectrum measured at -0.1Å^{-1}, i.e., an opposite wave vector to Fig. 4(c) relative to the $\overline{K}$ point. Figure 4(f) shows the counterpart of Fig. 4(e). All the measurement positions are marked on Fig. 4(b) by white lines, tilted due to a conversion from angles to wave vectors $k_\parallel$. (In the discussion we use approximate $k_\parallel$ values for simplicity.)

A comparison of opposite $k_\parallel$ values allows us to test for a spin-orbit (Rashba) contribution to the observed spin polarization following Fig. 1. Comparing Figs. 4(c) and 4(d) we see that the spectra are nearly identical. This is the direct indication of the absence of spin-orbit effects on Dirac cone spin splitting and spin polarization. As complementary information, we can directly prove the exchange-type nature by reversing the remanent magnetization of the sample. All features in the spin-resolved spectra reverse with the

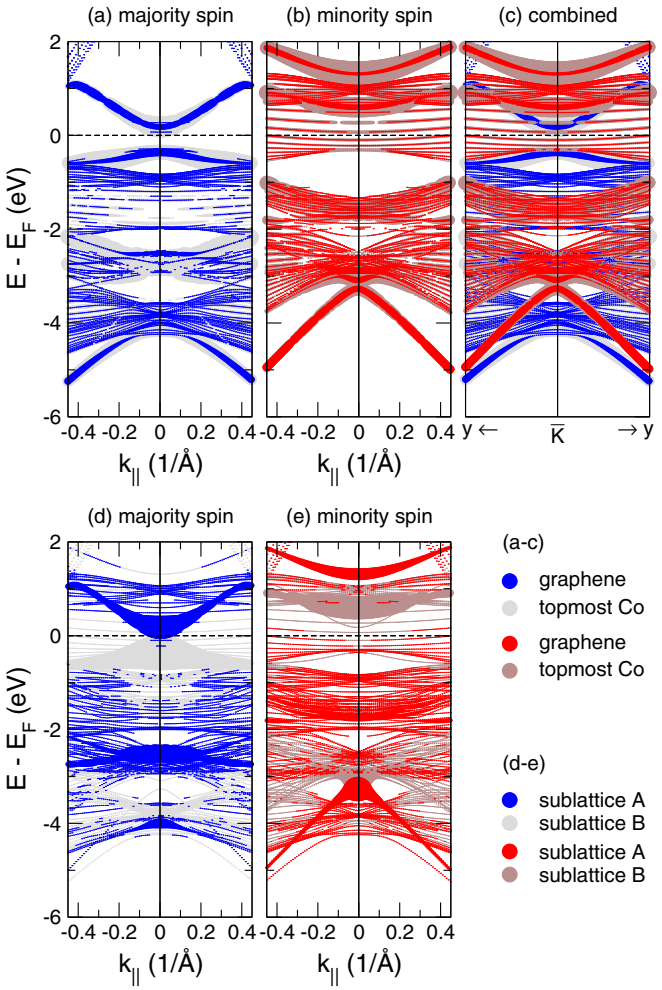

FIG. 5. (Color online) Band structure calculated for graphene/Co(0001) perpendicular to $\overline{\Gamma K}$. (a)–(c) Symbols indicate states with charge density on the carbon and at the topmost Co layer, i.e., the Co atomic layer in contact with the graphene. At $E - E_F = -3$ eV a Dirac crossing point is seen with strong weight at the graphene. This Dirac point and the lower half of the Dirac cone are situated in a minority-spin bulk band gap of the Co. (d), (e) Symbols indicate the sublattice polarization defined as $P = w(A) - w(B)$, where $w(X)$ is the local density of states (DOS) at atom X. The size of the symbol is determined by $|P|$ while the color is inferred by its sign.

magnetization, as shown for $\overline{K}$ and $+0.7\text{Å}^{-1}$ from $\overline{K}$ in the Supplemental Material [30,31] and in Fig. 4(h).

We have investigated the system graphene/Co(0001) by first-principles band-structure calculations. Figure 5 shows the results for a Co film covered on one side by graphene. Large symbol sizes indicate a high charge density at carbon and the topmost Co (interface) sites. The white areas correspond to surface-projected bulk band gaps. They are largely shifted by the exchange splitting of Co of about 1.6 eV. Therefore, only for minority spin do the lower Dirac cone and the Dirac crossing point (at −3.2 eV) lie in such a bulk band gap. The Dirac point can be investigated at a much smaller energy scale than in the experiment where the features are broad. The calculation shows a gap at the Dirac point of less than 200 meV. It is also seen that the graphene character is maintained below and above the Dirac point while the weight at the Co interface layer is overall larger at the Dirac point. The majority-spin part of the Dirac cone, instead, is degenerate with Co states near the Dirac point, has much more Co character there, and is spread over ∼0.5 eV width. This spin-dependent hybridization is able to withhold the minority-spin electrons at the graphene while the majority-spin electrons "leak" into the Co substrate. This contributes to an antiparallel magnetization there. The calculation confirms this impression and gives a magnetic moment at the on-top carbon site of $-0.032\mu_B$ and at the hollow carbon site of $+0.029\mu_B$ which gives a total carbon moment of $-0.003\mu_B$.

The minority-spin band at 1–1.5 eV from Fig. 4 is identified here as a minority-spin Co band (1.5–2.0 eV binding energy) at the interface. Also, the majority-spin state from the experiment (at ∼3 eV) is identified as the majority-spin Dirac point which is strongly hybridized. From Fig. 5(e) it is also seen that the exchange splitting of the graphene Dirac cone is positive (∼700 meV).

We have previously pointed out the importance of dynamic hybridization effects in graphene/Ni(111) [26]. This means that the hybridization is energy dependent. This is much more clearly revealed in graphene/Co due to the large exchange splitting in the Co. Figure 5(b) shows that the lower half of the Dirac cone at $E - E_F = -3$ eV already has graphene character while the upper half has a predominantly Co character. In the majority-spin panel [Fig. 5(a)] for the Dirac cone near the Fermi energy, it is the opposite.

This clearly confirms that almost intact Dirac cones can exist despite strong sublattice symmetry breaking. This is possible for k vectors slightly ($0.1\ \text{Å}^{-1}$) away from the $\overline{K}$ point because the upper and lower halves of the Dirac cones belong to different sublattices, as can be seen in Figs. 5(d) and 5(e). The separation of the Dirac cone into A and B sublattices is most pronounced directly at $\overline{K}$, where the two halves can mix effectively.

In summary, spin- and angle-resolved photoemission shows that graphene on Co(0001) forms a Dirac cone which is strongly minority-spin polarized. *Ab initio* calculations show that this spin polarization is due to a minority-spin bulk band gap of the Co, which hosts the lower half of the Dirac cone, including the Dirac point. This half cone is located at sublattice A and has a counterpart of majority spin. The majority-spin Dirac cone and the upper half of the minority spin Dirac cone are degenerate with Co bulk bands, which leads to a stronger Co character.

This physical insight that spin-polarized graphene Dirac cones form through spin-dependent bulk band gaps will be useful for interfacing graphene with metals as well as ferromagnetic insulators, and for combining exchange and spin-orbit interactions for realizing the quantum anomalous Hall effect in graphene.

Note added. Recently, we became aware of a study with similar conclusions, where the cone at the Fermi level is well resolved [37].

This work was supported by SPP 1459 of the Deutsche Forschungsgemeinschaft. G.B. is grateful for computing time on the JUROPA supercomputer at the Jülich Supercomputing Centre (JSC).

[1] N. Tombros, C. Jozsa, M. Popinciuc, H. T. Jonkman, and B. J. van Wees, Nature (London) **448**, 571 (2007).

[2] Wei Han, K. Pi, K. M. McCreary, Yan Li, Jared J. I. Wong, A. G. Swartz, and R. K. Kawakami, Phys. Rev. Lett. **105**, 167202 (2010).

[3] T.-Y. Yang, J. Balakrishnan, F. Volmer, A. Avsar, M. Jaiswal, J. Samm, S. R. Ali, A. Pachoud, M. Zeng, M. Popinciuc, G. Güntherodt, B. Beschoten, and B. Özyilmaz, Phys. Rev. Lett. **107**, 047206 (2011).

[4] W. Han and R. K. Kawakami, Phys. Rev. Lett. **107**, 047207 (2011).

[5] B. Uchoa, V. N. Kotov, N. M. R. Peres, and A. H. Castro Neto, Phys. Rev. Lett. **101**, 026805 (2008).

[6] V. M. Karpan, G. Giovannetti, P. A. Khomyakov, M. Talanana, A. A. Starikov, M. Zwierzycki, J. van den Brink, G. Brocks, and P. J. Kelly, Phys. Rev. Lett. **99**, 176602 (2007); V. M. Karpan, P. A. Khomyakov, A. A. Starikov, G. Giovannetti, M. Zwierzycki, M. Talanana, G. Brocks, J. van den Brink, and P. J. Kelly, Phys. Rev. B **78**, 195419 (2008).

[7] A. T. Ngo, J. M. Villas-Bôas, and S. E. Ulloa, Phys. Rev. B **78**, 245310 (2008).

[8] Q.-f. Sun, Z.-t. Jiang, Y. Yu, and X. C. Xie, Phys. Rev. B **84**, 214501 (2011).

[9] Q.-f. Sun and X. C. Xie, Phys. Rev. B **87**, 245427 (2013).

[10] H. X. Yang, A. Hallal, D. Terrade, X. Waintal, S. Roche, and M. Chshiev, Phys. Rev. Lett. **110**, 046603 (2013).

[11] H.-Ch. Mertins, S. Valencia, W. Gudat, P. M. Oppeneer, O. Zaharko, and H. Grimmer, Europhys. Lett. **66**, 743 (2004).

[12] J. Hong, E. Bekyarova, P. Liang, W. A. de Heer, R. C. Haddon, and S. Khizroev, Sci. Rep. **2**, 624 (2012).

[13] M. Weser, Y. Rehder, K. Horn, M. Sicot, M. Fonin, A. B. Preobrajenski, E. N. Voloshina, E. Goering, and Yu. S. Dedkov, Appl. Phys. Lett. **96**, 012504 (2010).

[14] Z. H. Qiao, S. A. Yang, W. X. Feng, W.-K. Tse, J. Ding, Y. G. Yao, J. Wang, and Q. Niu, Phys. Rev. B **82**, 161414(R) (2010).

[15] W.-K. Tse, Z. H. Qiao, Y. G. Yao, A. H. MacDonald, and Q. Niu, Phys. Rev. B **83**, 155447 (2011).

[16] Z. Qiao, H. Jiang, X. Li, Y. Yao, and Q. Niu, Phys. Rev. B **85**, 115439 (2012).

[17] J. Ding, Z. H. Qiao, W. X. Feng, Y. G. Yao, and Q. Niu, Phys. Rev. B **84**, 195444 (2011).

[18] H. B. Zhang, C. Lazo, S. Blügel, S. Heinze, and Y. Mokrousov, Phys. Rev. Lett. **108**, 056802 (2012).

[19] A. Varykhalov, J. Sánchez-Barriga, A. M. Shikin, C. Biswas, E. Vescovo, A. Rybkin, D. Marchenko, and O. Rader, Phys. Rev. Lett. **101**, 157601 (2008).

[20] I. Pletikosić, M. Kralj, P. Pervan, R. Brako, J. Coraux, A. T. N'Diaye, C. Busse, and T. Michely, Phys. Rev. Lett. **102**, 056808 (2009).

[21] A. Varykhalov, M. R. Scholz, Timur K. Kim, and O. Rader, Phys. Rev. B **82**, 121101(R) (2010).

[22] D. Marchenko, A. Varykhalov, M. R. Scholz, G. Bihlmayer, E. I. Rashba, A. Rybkin, A. M. Shikin, and O. Rader, Nat. Commun. **3**, 1232 (2012).

[23] D. Marchenko, J. Sánchez-Barriga, M. R. Scholz, O. Rader, and A. Varykhalov, Phys. Rev. B **87**, 115426 (2013).

[24] E. I. Rashba, Phys. Rev. B **79**, 161409(R) (2009).

[25] M. Gmitra, S. Konschuh, C. Ertler, C. Ambrosch-Draxl, and J. Fabian, Phys. Rev. B **80**, 235431 (2009).

[26] A. Varykhalov, D. Marchenko, J. Sánchez-Barriga, M. R. Scholz, B. Verberck, B. Trauzettel, T. O. Wehling, C. Carbone, and O. Rader, Phys. Rev. X **2**, 041017 (2012).

[27] O. Rader, A. Varykhalov, J. Sánchez-Barriga, D. Marchenko, A. Rybkin, and A. M. Shikin, Phys. Rev. Lett. **102**, 057602 (2009).

[28] Yu. S. Dedkov and M. Fonin, New J. Phys. **12**, 125004 (2010).

[29] G. C. Burnett, T. J. Monroe, and F. B. Dunning, Rev. Sci. Instrum. **65**, 1893 (1994).

[30] See Supplemental Material at http://link.aps.org/supplemental/10.1103/PhysRevB.91.235431 for more details on magnetization reversal, spectra fitting and comparison with ARPES from bare cobalt.

[31] D. Marchenko, Ph.D. thesis, Universität Potsdam, 2013, www.helmholtz-berlin.de/pubbin/oai_publication?VT=1&ID=84138.

[32] See http://www.flapw.de for a program description.

[33] I. Hamada and M. Otani, Phys. Rev. B **82**, 153412 (2010).

[34] E. L. Shirley, L. J. Terminello, A. Santoni, and F. J. Himpsel, Phys. Rev. B **51**, 13614 (1995).

[35] A. Bostwick, Progr. Surf. Sci. **84**, 380 (2009).

[36] D. Pacilé, S. Lisi, I. Di Bernardo, M. Papagno, L. Ferrari, M. Pisarra, M. Caputo, S. K. Mahatha, P. M. Sheverdyaeva, P. Moras, P. Lacovig, S. Lizzit, A. Baraldi, M. G. Betti, and C. Carbone, Phys. Rev. B **90**, 195446 (2014).

[37] D. Usachov, A. Fedorov, M. M. Otrokov, A. Chikina, O. Vilkov, A. Petukhov, A. G. Rybkin, Y. M. Koroteev, E. V. Chulkov, V. K. Adamchuk, A. Grüneis, C. Laubschat, and D. V. Vyalikh, Nano Lett. **15**, 2396 (2015).